

Nonlinear Resonant Transport of Bose-Einstein Condensates

Tobias Paul, Klaus Richter, and Peter Schlagheck

Institut für Theoretische Physik, Universität Regensburg, 93040 Regensburg, Germany
(April 14, 2024)

The coherent flow of a Bose-Einstein condensate through a quantum dot in a magnetic waveguide is studied. By the numerical integration of the time-dependent Gross-Pitaevskii equation in presence of a source term, we simulate the propagation process of the condensate through a double barrier potential in the waveguide. We find that resonant transport is suppressed in interaction-induced regimes of bistability, where multiple scattering states exist at the same chemical potential and the same incident current. We demonstrate, however, that a temporal control of the external potential can be used to circumvent this limitation and to obtain enhanced transmission near the resonance on experimentally realistic time scales.

PACS numbers: 03.75.Dg, 03.75.Kk, 42.65.Pc

The rapid progress in the fabrication and manipulation of ultracold Bose-Einstein condensates has lead to a number of fascinating experiments probing complex condensed matter phenomena in perfectly controllable environments, such as the creation of vortex lattices [1] and the quantum phase transition from a superfluid to a Mott insulator state in optical lattices [2]. With the development of "atom chips" [3-5], new perspectives are opened also towards mesoscopic physics. The possibility to generate atomic waveguides of arbitrary complexity above microfabricated surfaces does not only permit highly accurate matter-wave interference experiments [6], but would also allow to study the interplay between interaction and transport with an unprecedented degree of control of the involved parameters. The connection to electronic mesoscopic physics was appreciated by Thywissen et al. [7] who proposed a generalization of Landauer's theory of conductance [8] to the transport of non-interacting atoms through point contacts. Related theoretical studies were focused on the adiabatic propagation of a Bose-Einstein condensate in presence of obstacles [9-12], the dynamics of soliton-like structures in waveguides (e.g. [13]), and the influence of optical lattices on transport (e.g. [14]), to mention just a few examples.

Particularly interesting in this context is the propagation of a Bose-Einstein condensate through a double barrier potential, which can be seen as a Fabry-Pérot interferometer for matter waves. In the context of atom chips, such a bosonic quantum dot could be realized by suitable geometries of microfabricated wires. An alternative implementation based on optical lattices was suggested by Carusotto and La Rocca [15,16] who pointed out that the interaction-induced nonlinearity in the mean-field dynamics would lead to a bistability behaviour of the transmitted flux in the vicinity of resonances. This phenomenon is well known from nonlinear optics [17] and arises also in electronic transport through quantum wells (e.g. [18-20]) due to the Coulomb interaction in the well.

In this Letter, we investigate to which extent resonant transport through such a double barrier potential can

be achieved for an interacting condensate in a realistic propagation process, where the magnetic guide is gradually filled with matter wave. To simulate such a process, we numerically integrate the time-dependent Gross-Pitaevskii equation in presence of a source term that models the coupling to a reservoir of Bose-Einstein condensed atoms. We shall point out that resonant scattering states, which exist in principle for arbitrarily strong interactions, cannot be populated in the above way if the nonlinearity induces a bistability regime near the resonance. Finally, we suggest an adiabatic control scheme that permits to circumvent this limitation on experimentally feasible time scales.

We consider a coherent beam of Bose-Einstein condensed atoms propagating through a double barrier potential in a magnetic waveguide. In presence of a strong cylindrical confinement with trapping frequency ω_\perp , the mean-field dynamics of the condensate is described by the effective one-dimensional Gross-Pitaevskii equation

$$i\hbar \frac{\partial \psi}{\partial t} = -\frac{\hbar^2}{2m} \frac{\partial^2 \psi}{\partial x^2} + V(x) + g|\psi(x;t)|^2 \psi(x;t) \quad (1)$$

with $g = 2a_s\hbar^2/m$ [21], where m is the mass and a_s the s-wave scattering length of the atoms. For the sake of definiteness, the double barrier potential is given by

$$V(x) = V_0 \frac{\hbar^2}{m} \frac{e^{-(x+L/2)^2/\lambda^2} + e^{-(x-L/2)^2/\lambda^2}}{2} \quad (2)$$

(see Fig. 1). Our numerical calculations were performed for ^{87}Rb atoms ($a_s = 5.77\text{nm}$) with $\omega_\perp = 2 \cdot 10^3\text{s}^{-1}$, $a_\perp = \hbar/m\omega_\perp = 0.34\text{nm}$, $V_0 = \hbar^2/\lambda^2$, and $L = 10 \cdot a_\perp = 3.4\text{nm}$ [22]. This yields $g = 0.034\hbar^2/m a_\perp$.

Let us first discuss resonances in terms of stationary scattering states of the condensate. The latter are given by stationary solutions $\psi(x;t) = \psi(x) \exp(-iEt/\hbar)$ of Eq. (1) satisfying outgoing boundary conditions of the form $\psi(x) = A e^{ikx}$ with $k > 0$ for $x \rightarrow \pm 1$. To calculate them, we insert the ansatz $\psi(x) = A(x) \exp[i\phi(x)]$ (with real A and ϕ) into the stationary Gross-Pitaevskii

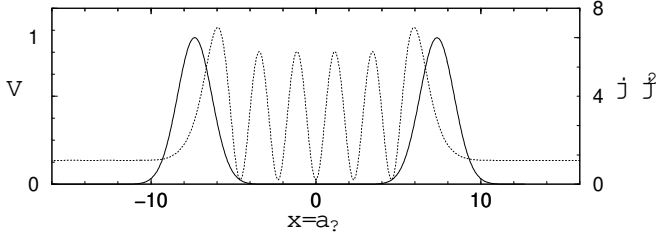


FIG. 1. External longitudinal potential V in units of \hbar^2/a_2^2 . The dotted line shows the longitudinal atom density (in units of a_2^{-1}) of the scattering state associated with the 5th excited resonance, calculated at $\mu = 1.127\hbar^2/a_2^2$ and $j_z = 1.6\hbar^2/a_2^2$.

equation, and separate the latter into real and imaginary parts. This yields the condition that the current $j(x) = (\hbar/m)A^2(x)\phi'(x)$ is independent of x , and

$$A = \frac{\hbar^2}{2m} \frac{d^2 A}{dx^2} + V(x)A + \frac{m}{2} \frac{j_z^2}{A^4} A + gA^3 \quad (3)$$

a equation for the amplitude $A(x)$. The latter can be numerically integrated from the "downstream" ($x \rightarrow -\infty$) to the "upstream" ($x \rightarrow \infty$) region by means of a Runge-Kutta solver. As "asymptotic condition" at $x \rightarrow \infty$, we choose $A' = 0$ and A satisfying

$$= \frac{m}{2} \frac{j_z^2}{n^2} + gn; \quad (4)$$

for a given j_z , with $n = A^2$ the longitudinal density of the condensate. As was pointed out in Ref. [9], Eq. (4) exhibits a low-density (supersonic) and a high-density (subsonic) solution, where the transport is respectively dominated by the kinetic energy and by the mutual interaction of the atoms. Since in realistic propagation processes the waveguide is initially empty in the downstream region, we choose the low-density solution for the asymptotic value of A .

A measure of the proximity of the scattering state to a resonant state is provided by the drag

$$F_d = \sum_{n=1}^{Z+1} \int dx n(x) \frac{dV(x)}{dx} \quad (5)$$

that the condensate exerts onto the obstacle [11]. Far from any resonance, the amount of reflection from the potential is rather large, leading to a finite drag due to the associated momentum transfer, while a vanishing drag is expected near a resonance where the condensate is perfectly transmitted through the quantum dot. In Fig. 2, the drag is plotted as a function of μ and j_z in the vicinity of the 5th and 6th excited resonance, which have five and six nodes within the well, respectively (see Fig. 1). While the chemical potential of the resonant

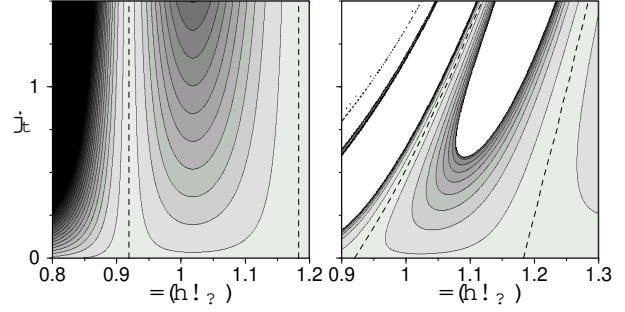


FIG. 2. Drag exerted by the condensate onto the obstacle, plotted as a function of the chemical potential μ and the total current j_z (in units of \hbar^2/a_2^2) for $g = 0$ (left panel) and $g = 0.034\hbar^2/a_2^2$ (right panel). Light gray areas correspond to a low and dark gray areas to a high drag. In white areas, the integration of Eq. (3) leads to a diverging $A(x)$. The location of the 5th and 6th excited resonance, where the drag vanishes, is marked by dashed lines.

state is independent of j_z in the linear case, it increases with j_z in presence of a repulsive atom-atom interaction. Note that for large currents scattering states with non-diverging amplitude $A(x)$ exist only in the immediate vicinity of resonances.

Can resonant scattering states be populated in a realistic experiment where the condensate is initially confined in a microtrap and then released to propagate through the waveguide? To address this question, we numerically integrate the time-dependent Gross-Pitaevskii equation

$$i\hbar \frac{\partial}{\partial t} \psi(x;t) = \frac{\hbar^2}{2m} \frac{\partial^2}{\partial x^2} \psi(x;t) + V(x) \psi(x;t) + g|\psi(x;t)|^2 \psi(x;t) + S_0 \exp(-i\hbar t) \delta(x - x_0) \quad (6)$$

in presence of an inhomogeneous source term emitting coherent matter waves with chemical potential μ at position x_0 (we used $x_0 = 15a_2$ in our calculation). The wavefunction $\psi(x;t)$ is expanded on a lattice (within $-20 \leq x/a_2 \leq 20$) and propagated in real time domain. To avoid artificial backscattering from the boundaries of the lattice, we impose absorbing boundary conditions which are particularly suited for transport problems [23] and can be generalized to account for weak or moderate nonlinearities [24,25].

Stationary scattering states can now be calculated by propagating $\psi(x;t)$ in presence of an adiabatic increase of the source amplitude S_0 from 0 up to a given maximum value, with the initial condition $\psi = 0$. This approach simulates a realistic propagation process where a coherent beam of Bose-Einstein condensed atoms with chemical potential μ is injected into the guide from a reservoir. Furthermore, it provides a straightforward access to the

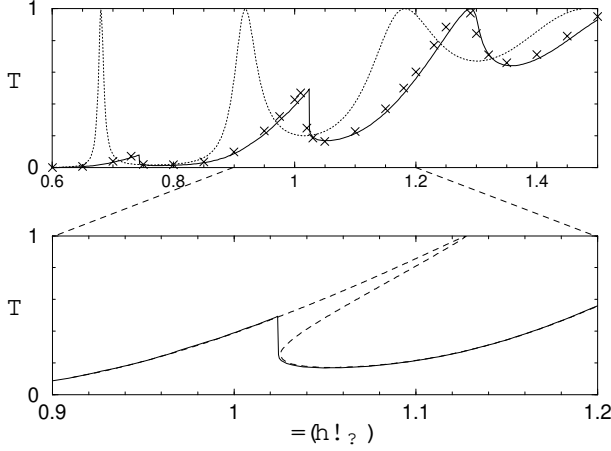


FIG. 3. Transmission spectrum obtained from the time-dependent propagation approach for $g = 0.034\hbar^{-1}a_0$ and fixed incident current $j_i = 1.6!$ (solid line) compared, in the upper panel, to the interaction-free spectrum (dotted line). The crosses show the results of a full three-dimensional calculation [24]. The dashed line in the lower panel shows the two other branches of the 5th resonance peak, which are not populated by the time-dependent propagation process.

transmission coefficient T that is associated with a given scattering state: T can be defined by the ratio of the current j_t in presence of the double barrier potential (i.e., the transmitted current) to the current j_i obtained in absence of the potential (the incident current). The latter is analytically evaluated as $j_i = \hbar \int_0^\infty j = (\hbar k_0) w$ with k_0 being self-consistently defined by $k_0 = \frac{2m}{\hbar} \sqrt{g \int_0^\infty j = k_0^2} = \hbar$.

Fig. 3 shows the transmission coefficient as a function of the chemical potential around the 5th excited resonance. For each value of μ , the wavefunction was propagated according to Eq. (6) in presence of an adiabatic increase of the source amplitude S_0 up to the maximum value that corresponds to the incident current $j_i = 1.6!$. The transmitted current is directly evaluated from the stationary scattering state obtained at the end of the propagation procedure. While the typical sequence of Breit-Wigner resonances is obtained in the linear case (or in the limit of very low incident currents), the profiles become asymmetric for $g > 0$ with perfect transmission being suppressed for narrow resonances. These results are essentially reproduced by a full three-dimensional mean-field calculation, which will be described elsewhere [24].

The step-like structures in the transmission spectrum indicate a bistability phenomenon, as known from similar processes in nonlinear optics [17] and in electronic transport through quantum wells (e.g. [18(20)]). Additional branches of the resonance peaks are indeed identified by

the integration method based on Eq. (3) which allows to calculate stationary scattering states for given j_t and μ . The incident current of the scattering state is approximately determined according to Ref. [12] via

$$j_i = \frac{\hbar}{2m} \frac{gn_{av}}{(n_{av} + \frac{p}{n_{max}n_{min}})} \quad (7)$$

with $n_{av} = \frac{1}{2}(n_{max} + n_{min})$, where n_{max} and n_{min} denote them maxima and minima, respectively, of the longitudinal upstream density. The expression (7) assumes a cosine-like oscillation of the upstream density, and is valid for small $g(n_{max} - n_{min}) = n_{av}$.

Finding the value of j_t that results from a given j_i is now an optimization problem that can be solved straightforwardly. The result is shown in the lower panel of Fig. 3 for chemical potentials around the 5th resonant state. In addition to the spectrum obtained by the integration Eq. (6), two further solutions appear for $1.02 < \mu < 1.13$ which join together to form a resonance peak that is asymmetrically distorted towards higher μ . The existence of such a multivalued spectrum, which is reminiscent of nonlinear oscillators, was in this context pointed out by Carusotto and La Rocca [15]. Since the additional branches of the resonance peak are apparently not populated by the time-dependent integration approach, we expect that resonant transport will generally be suppressed in a realistic propagation process. Loosely speaking, the atoms "block" each other when going through the double barrier potential [26].

To enhance the transmission of matter waves near a narrow resonance, the external potential needs to be varied during the propagation process. Specifically, this can be achieved e.g. by illuminating the scattering region with a red-detuned laser pulse. We can describe such a process by a temporal modulation of V according to

$$V(x) \rightarrow V(x;t) = V(x) + V_0(t) \quad (8)$$

where $V_0(t) > 0$ is determined by the detuning and the time-dependent intensity of the laser. For an adiabatic modulation of V , the wavefunction $\psi(x;t)$ will, at each time t , remain close to the instantaneous scattering state associated with the external potential (8) — or, equivalently formulated, to the scattering state for $V = V(x) + V_0(t)$. Outside the bistability regime, e.g. for $\mu + V_0(t) < 1.02\hbar^{-1}$ in case of the 5th resonance, this scattering state would be uniquely given by the one that is also obtained by the direct propagation process. However, as soon as the effective chemical potential $\mu + V_0(t)$ is raised above $1.02\hbar^{-1}$, the wavefunction will continuously follow the upper branch of the resonance and evolve into a near-resonant scattering state with high transmission.

Indeed, we can use our numerical setup to simulate such a process. Fig. 4 shows the transmission coefficient as a function of the propagation time, where the effective

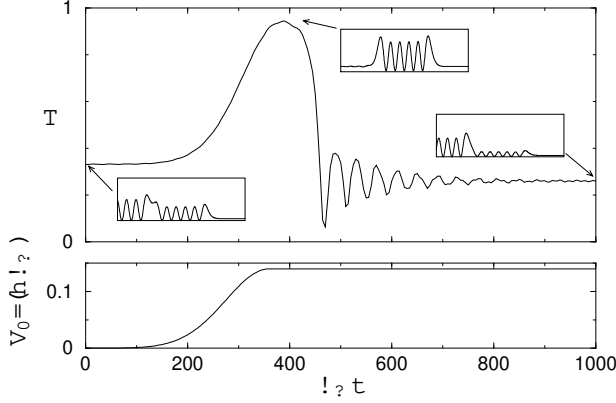


FIG. 4. Time evolution of the transmission coefficient T (upper panel) during the ramping process of the external potential V_0 (lower panel) which shifts the effective chemical potential from $\mu = 0.985\hbar\omega_c$ to $1.125\hbar\omega_c$. As shown in the insets (with scaling as in Fig. 1), the wavefunction adiabatically evolves into a nearly resonant state with transmission close to unity, and decays from there to the low-transmission scattering state within a time scale of the order of $100\hbar\omega_c^{-1}$.

chemical potential was shifted from $\mu = 0.985\hbar\omega_c$ to $\mu + V_0^{\text{max}} = 1.125\hbar\omega_c$ by means of a Gaussian ramping process taking place within $0 < \hbar t < 360$ (see the lower panel of Fig. 4). We see that the transmission approaches unity at the end of the ramping process, which clearly indicates that the scattering wavefunction evolves along the upper branch of the resonance peak. This is indeed confirmed by the associated density shown in the insets (to be compared with Fig. 1).

As was also pointed out in the context of electronic transport through quantum wells [20], the resonant scattering state is dynamically unstable in presence of interactions. This instability is indeed encountered in our system: Continuing the numerical propagation beyond $\hbar t = 360$ (at fixed V_0) results in a decay of the wavefunction towards a low-transmission scattering state within a time scale of the order of $100\hbar\omega_c^{-1}$, i.e. 16 ns . This lifetime should be long enough, however, to transport a large fraction of the condensate through the double barrier, as well as to manipulate the resonant scattering state: by closing, for instance, the potential well during that time scale (e.g. with blue-detuned lasers that enhance the potential outside the barriers), one would create a trap in which an interacting many-body state with an unusually high excitation (with five nodes in case of the 5th excited resonance) would be obtained.

In conclusion, we have studied resonant transport of interacting Bose-Einstein condensates through a symmetric double barrier potential in a magnetic waveguide. The

nonlinearity induced by the interaction leads to a distortion of the resonance peak, where the associated scattering state cannot be populated by directly sending coherent matter wave onto the initially empty waveguide. To obtain nevertheless a finite amount of transmission on intermediate time scales, the external potential needs to be adiabatically varied during the propagation process. The lifetime of the resonant scattering state obtained in this way is predicted to be of the order of 10 ns for our particular setup, which should be long enough to allow for further experimental manipulations. We expect that the basic principles of the scenario encountered for our double barrier potential apply also to more complex quantum dot geometries such as sequences of more than two barriers along the guide. This indicates that the design of suitable control schemes will be a relevant issue for the mesoscopic transport of Bose-Einstein condensates.

It is a pleasure to thank Nicolas Pavloff, Peter Schmelcher, Joachim Brand, Jozsef Fortagh, and Wilhelm Prettl for fruitful and inspiring discussions.

-
- [1] J. R. Abo-Shaeer, C. Raman, J. M. Vogels, and W. Ketterle, *Science* **292**, 476 (2001).
 - [2] M. Greiner et al., *Nature* **415**, 39 (2002).
 - [3] R. Fomby et al., *Phys. Rev. Lett.* **84**, 4749 (2000).
 - [4] H. Ott et al., *Phys. Rev. Lett.* **87**, 230401 (2001).
 - [5] W. Hansel, P. Hommelho, T. W. Hansch, and J. Reichel, *Nature* **413**, 498 (2001).
 - [6] E. Andersson et al., *Phys. Rev. Lett.* **88**, 100401 (2002).
 - [7] J. H. Thywissen, R. M. Westervelt, and M. Prentiss, *Phys. Rev. Lett.* **83**, 3762 (1999).
 - [8] D. K. Ferry and S. M. Goodnick, *Transport in Nanostructures* (Cambridge University Press, Cambridge, 1997).
 - [9] P. Leboeuf and N. Pavloff, *Phys. Rev. A* **64**, 033602 (2001).
 - [10] M. Jaaskelainen and S. Stenholm, *Phys. Rev. A* **66**, 023608 (2002).
 - [11] N. Pavloff, *Phys. Rev. A* **66**, 013610 (2002).
 - [12] P. Leboeuf, N. Pavloff, and S. Sinha, *Phys. Rev. A* **68**, 063608 (2003).
 - [13] S. Komineas and N. Papanicolaou, *Phys. Rev. Lett.* **89**, 070402 (2002).
 - [14] K. M. Hilligs, M. K. Oberthaler, and K.-P. Marzlin, *Phys. Rev. A* **66**, 063605 (2002).
 - [15] I. Carusotto and G. C. La Rocca, *Phys. Rev. Lett.* **84**, 399 (1999).
 - [16] I. Carusotto, *Phys. Rev. A* **63**, 023610 (2001).
 - [17] R. W. Boyd, *Nonlinear Optics* (Academic Press, London, 1992).
 - [18] V. J. Goldmann, D. C. Tsui, and J. E. Cunningham, *Phys. Rev. Lett.* **58**, 1256 (1987).
 - [19] C. Presilla, G. Jona-Lasinio, and F. Capasso, *Phys. Rev. B* **43**, 5200 (1991).
 - [20] M. Y. Azbel, *Phys. Rev. B* **59**, 8049 (1999).
 - [21] M. Olshanii, *Phys. Rev. Lett.* **81**, 938 (1998).
 - [22] Such a small barrier width would be at the limit of real-

izability with present-day atom-chip technology. We remark, however, that the phenomena we discuss here do not sensitively depend on the chosen parameters nor on the specific shape of the potential.

- [23] T. Shibata, Phys. Rev. B 43, 6760 (1991).
- [24] T. Paul, P. Schlagheck, and K. Richter, in preparation.
- [25] We reproduced our results by an alternative approach using complex absorbing potentials at the boundaries.
- [26] This phenomenon must not be confused with the "atom blockade" discussed by Carusotto [16], which arises in the limit of few atoms and very strong interactions.